Convergence of the hole-line expansion with modern nucleon-nucleon potentials

Jia-Jing Lu (陆家靖), Zeng-Hua Li (李增花),[*] and Chong-Yang Chen (陈重阳)

Department of Nuclear Science and Technology, Institute of Modern Physics, Fudan University,
Shanghai 200433, People's Republic of China

M. Baldo and H.-J. Schulze

Dipartimento di Fisica, INFN Sezione di Catania, Universitá di Catania, Via Santa Sofia 64, 95123 Catania, Italy

We calculate the three-hole-line contributions to the binding energy of symmetric nuclear matter in the Brueckner-Bethe-Goldstone expansion using various modern nucleon-nucleon potentials of high precision. The relation with the correlation parameter $\kappa = \rho V_{\text{core}}$ is examined. In all cases the three-hole-line contributions turn out to be sufficiently small, but no satisfactory saturation is obtained. This means that three-nucleon forces are essential for all considered potentials.

I. INTRODUCTION

The accurate computation of the binding energy and related properties of bulk nuclear matter is a long-lasting theoretical problem [1–3] that received new impetus from the recent activity in the field of chiral perturbation theory [4]. The basic difficulty stems from the fact that traditional nucleon-nucleon forces [(NN) potentials] feature a very strong repulsion at short distances, i.e., a "hard core," caused by the quark substructure of the nucleons. This renders a straightforward perturbative calculation impossible.

Various theoretical approaches have been devised to confront this problem. In this article we employ the Brueckner-Bethe-Goldstone (BBG) theory of dense Fermi systems [5] in which the expansion parameter $\kappa = (c/d)^3$ is given by the cubed ratio of the short-range (hard-core) interaction range c to the average interparticle distance d [6,7]. This translates into an expansion in terms of hole lines of the associated Goldstone diagrams, for example, the binding energy per particle of symmetric nuclear matter (SNM) can be written as

$$B/A = T + E_2 + E_3 + \cdots, \qquad (1)$$

where T is the kinetic energy, $E_2 = E_{\text{BHF}}$ is the two-hole-line (2HL) contribution at the Brueckner-Hartree-Fock (BHF) level, and E_3 is the three-hole-line (3HL) contribution, which will be the main focus of this article.

In Ref. [7] we have recently analyzed the density dependence of the correlation parameter κ for various modern NN potentials, including recent chiral potentials. We found distinct qualitative differences between the potentials, related to the condition whether a strong hard core is present (r-space potentials) or not (chiral potentials). In the latter case the hole-line expansion (HLE) parameter κ becomes very small with increasing density. On the other hand, in the absence of a hard core, i.e., a dominant short-range interaction, the very justification of the HLE becomes doubtful. Therefore, in this new paper we continue our previous study by explicitly computing the 3HL contributions to the binding energy of

symmetric nuclear matter in the BBG expansion presenting and comparing results obtained with the Argonne V18 (AV18) [8], the CDBONN [9], and the recent N3LO chiral potentials [10] with two values of the chiral cutoff $\Lambda = 450,500$ MeV.

A further important check of the convergence of the HLE is the comparison of results obtained with different choices of the BHF auxiliary single-particle (s.p.) potential $U(k)$, usually the "continuous" and "gap" choices, and we will also perform this comparison.

II. FORMALISM

A. Correlation parameter and hole-line expansion

In Ref. [7] we related the correlation parameter κ of symmetric nuclear matter to the BHF defect function η in the following way [5,11]:

$$\kappa = \rho \int d^3\boldsymbol{r} \langle |\eta(\boldsymbol{r})|^2 \rangle_{S,T} = N\frac{V_{\text{core}}}{V} = \left(\frac{c}{d}\right)^3, \qquad (2)$$

which expresses the correlation parameter as the ratio of the core (or "wound") volume to the volume per particle, or equivalently, the cubed ratio of core diameter c to average nucleon distance d. Since the core volume or diameter defined in this way from the density-dependent defect functions are not constant, but in general shrink with increasing density, the result is a nonlinear density dependence of the correlation parameter κ as illustrated in Fig. 3(d).

It was shown explicitly in Ref. [7] that the competition between the long-range $^3SD_1$ deuteron partial wave and the other more short-range channels determines the overall density dependence of the correlation strength $\kappa = \sum_\alpha \kappa_\alpha$ for the different potentials. For soft potentials (N3LO) all correlation volumes and even the parameters κ_α disappear fast with increasing density, whereas for hard potentials (AV18) the correlation strength might increase again with density due to the dominance of the persistent p-wave contributions at high densities. This is seen in Fig. 3(d).

Equation (2) has the following interpretation as the foundation of the HLE: For a system with interaction range c and average particle distance $d > c$, the probability of finding a cluster of n interacting (correlated) particles is $(c/d)^{3n} = \kappa^n \ll 1$.

---

[*]zhli09@fudan.edu.cn

This suggests grouping the energy diagrams according to the number of interacting particles—first two-body correlations or clusters, then three-body correlations, etc. The number of interacting particles is equivalent to the number of hole lines, so this leads to the HLE Eq. (1), which amounts to an expansion in density governed by the dimensionless parameter $\kappa = \rho V_{\text{core}}$. However, this assertion obviously hinges on the condition that the dominant component of the interaction is the short-range core part and therefore in practice the convergence of the HLE should be verified for any potential by explicit computation, which is the purpose of the present article.

B. The 3HL contributions to the binding energy

In the BBG expansion the bare NN two-body interaction V systematically is replaced by the G matrix, which satisfies the Bethe-Goldstone equation,

$$\langle 12|G(W)|1'2'\rangle = \langle 12|V|1'2'\rangle - \sum_{1''2''}\langle 12|V|1''2''\rangle$$

$$\times \frac{Q}{E-W}\langle 1''2''|G(W)|1'2'\rangle, \qquad (3)$$

where each variable $1,\dots$ stands for $(\boldsymbol{k},\sigma,\tau)_1$, i.e., the three-dimensional momentum $\boldsymbol{k}$ and the spin-isospin variables σ,τ. Antisymmetrization of the matrix elements always is understood. The energy W is the so-called entry energy, which appears as a parameter in the equation. The Pauli operator Q projects the intermediate states $1'',2''$ with energy E above the Fermi momenta. As is well known, the G matrix sums up the ladder diagrams in the particle-particle scattering and takes into account most of the short-range correlations introduced by the hard core of the interaction if present. It is therefore much softer than the original bare interaction, and an expansion in the G matrix is expected to have an improved rate of convergence.

In the BBG expansion the diagrams then are grouped according to the order of the correlations that they are expected to describe. It turns out that this is equivalent to group the diagrams according to the number of hole lines that they contain. For an introduction to the subject, see Ref. [2] and the references therein. To sum up the diagrams at a given order of correlations it is quite useful to introduce a hierarchy of in-medium scattering matrices. With the G matrix one can sum up the two-body correlation diagrams, depicted in Figs. 1(a) and 1(b).

For the three-body correlations one introduces the three-body in-medium scattering matrix $T^{(3)}$, Fig. 1(g), which satisfies the Bethe-Fadeev equations, which are the analogs of the Fadeev equations for the three-body scattering matrix in free space. Because of antisymmetry, the original three coupled equations for distinguishable particles reduce to a single equation [2],

$$\langle 123|T^{(3)}|1'2'3'\rangle = \langle 12|G|1'2'\rangle\delta_{33'} - \sum_{1''2''3''}\langle 123|GX|1''2''3''\rangle$$

$$\times \frac{Q_3}{E_3 - W_3}\langle 1''2''3''|T^{(3)}|1'2'3'\rangle. \qquad (4)$$

The factor $Q_3/(E_3 - W_3)$ is the analog of the factor $Q/(E - W)$ appearing in the integral equation for the two-body
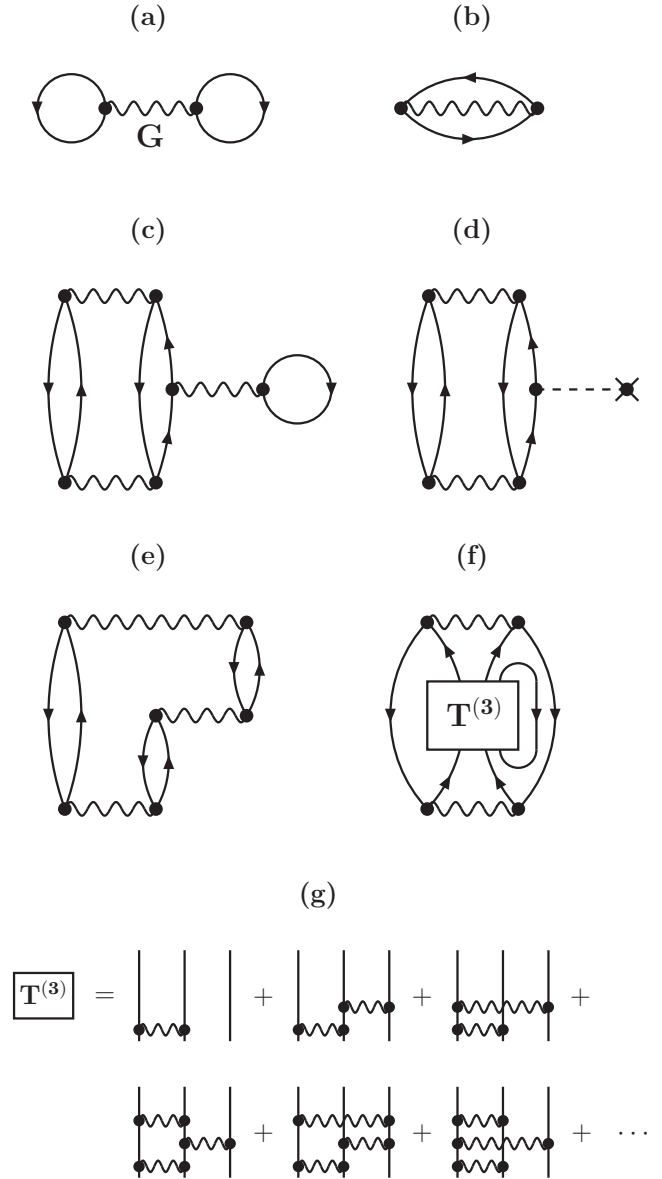

FIG. 1. Different Goldstone diagrams contributing to the binding energy of nuclear matter. Diagrams (a) and (b) correspond to the BHF calculation. The sum of the other diagrams (c)–(f) gives the three-hole-line contribution. The expansion of the Bethe-Fadeev integral equation is sketched in (g). For more details, please see the text.

scattering matrix G, namely, the projection operator Q_3 imposes that all the three-particle states lie above the Fermi energy and E_3 in the denominator is the energy of the three-particle intermediate state, in close analogy with the equation for the two-body scattering matrix.

The real novelty with respect to the two-body case is the operator $X = P_{123} + P_{132}$, where P indicates the operation of cyclic permutation of its indices. This operator interchanges particle 3 with particles 1 or 2. It gives rise to the so-called "endemic factor" in the Fadeev equations since it is an unavoidable complication intrinsic to the three-body problem in general. The reason for the appearance of the operator X in this context is that no two successive G matrices can be

present in the same pair of particle lines since the G matrix already sums up all the two-body ladder processes. In other words, the G matrices must alternate from one pair of particle lines to another in all possible ways, as is indeed apparent from the expansion by iteration of Eq. (4), sketched in Fig. 1(g).

The three-body scattering matrix $T^{(3)}$ appears in the schematic diagram of Fig. 1(f), which indeed sums up all the irreducible scattering processes among three particles in the medium. However, for numerical reasons it is useful to separate the lowest-order diagram of the series, depicted in Fig. 1(c), which is usually indicated as a "bubble diagram." It features a slow rate of convergence with respect to the sum over the angular momentum that characterizes the G matrix on the right-hand side of the diagram due to the long range of the one-pion-exchange interaction. The summation must then be extended to high angular momentum. The higher-order diagrams do not present such a problem, and the involved angular momenta can be restricted to relatively low values.

The exchange diagram of the bubble diagram is the "ring diagram" of Fig. 1(e). It describes the effect of the long-range correlations. The contribution of the higher-order diagrams of the particle-hole ladder series, i.e., diagrams with more than one particle-hole bubble, seems to be negligible [12] in nuclear matter. Long-range correlations also are embodied in the hole-hole propagation, which can be considered together with the particle-particle propagation of the Brueckner G matrix. The hole-hole contributions can be relevant for the nuclear matter binding energy, in particular in the self-consistent Green's function approach [13–16]. However, both series of higher-order diagrams include an arbitrary number of hole lines, and they would be in contrast with the hole-line BBG expansion, which suggests that all the diagrams with a given number of hole lines must be grouped together to minimize their contribution.

Finally the diagram of Fig. 1(d) is the first "potential insertion" diagram. This is the first of a series of additional diagrams that are a relevant and distinct feature of the BBG expansion: In the BBG scheme one introduces an auxiliary s.p. potential U, which modifies the s.p. spectrum. The Hamiltonian H is thus split as follows:

$$H = (T + U) + (V - U),\qquad(5)$$

where T is the kinetic energy. In the BBG expansion one then uses as the s.p. Hamiltonian $T + U$ and as the interaction $V - U$. Besides the original two-body interaction V one then obtains a set of contributions from the interaction term $-U$. Because the splitting of Eq. (5) is just an identity, the final result, after summing the diagrams to all orders, is formally independent of U. However, the introduction of U is expected to speed up the convergence of the expansion since with a proper choice of the mean-field U the interaction $V - U$ can be made much weaker than the original interaction V. In other words, the s.p. potential U effectively can incorporate a major fraction of the correlations.

A possible and physically motivated choice of the potential, which turned out to be quite convenient, is the so-called "Brueckner potential," which is defined in terms of the G

matrix,

$$U(1) = \sum_2 \langle 12|G(e_1 + e_2)|12\rangle,\qquad(6)$$

where

$$e_1 = \frac{k_1^2}{2m_1} + U(1)\qquad(7)$$

is the s.p. spectrum. Equations (6) and (7) imply a self-consistent procedure for the calculation of the s.p. potential $U(k)$. Once the potential is obtained, the 3HL diagrams and higher are calculated using the s.p. spectrum of Eq. (7).

At the 2HL level of approximation the energy per particle is given by

$$E_2 = \frac{1}{2A} \sum_{12} n(1)n(2)\langle 12|G(e_1 + e_2)|12\rangle,\qquad(8)$$

where $n(k) = \theta(k_F - k)$ is the occupation number for the free Fermi gas. This restricts the summations inside the Fermi sphere. The 3HL contribution is obtained in an analogous way. In particular, the diagonal matrix element of the three-particle scattering matrix has to be integrated over the three external momenta. In addition the diagram of Fig. 1(d), not directly connected with $T^{(3)}$, must be added. The calculations are very complex, and the explicit expressions for the 3HL diagrams can be found in Refs. [2,12,17].

A remark on the choice of Eq. (6) for the s.p. potential is in order. This definition is actually not unique. In the so-called standard choice, or "gap choice," the potential is assumed to be zero above the Fermi momenta so that the self-consistent procedure is carried out only below the Fermi momentum. In the "continuous choice" the definition of Eq. (6) is extended to all momenta, and the self-consistency then is demanded for arbitrary values of the momenta. The two choices give of course quite different s.p. potentials. However, as already noticed, the final result obtained summing up the diagrams to all orders must be independent of the choice of U. The possible independence of the results from U at a given order of approximation can be taken as a criterion for the convergence of the expansion and an estimate of the theoretical error.

Extensive results up to the 3HL order with the gap choice for the Reid and V_{14} potentials can be found in Refs. [12,18–20]. The first complete calculations with the continuous choice were given in Refs. [21–23] where indeed the approximate independence from the choice of U once the 3HL contributions are included was explicitly demonstrated. For the employed Argonne V_{14} and V_{18} NN interactions, the 3HL contribution in the continuous choice was found quite small. Later also results with the CDBONN [24], the Argonne $V_{8,6,4}$ [15], and the fss2 [25] potentials were presented.

In the following we will focus on the confrontation of the representative AV18 and CDBONN results with new ones for the chiral N3LO potentials and study the consistency with the hole-line parameter κ.

III. RESULTS

As a first illustration, we plot in Fig. 2 the saturation curves for SNM obtained with the different potentials at the
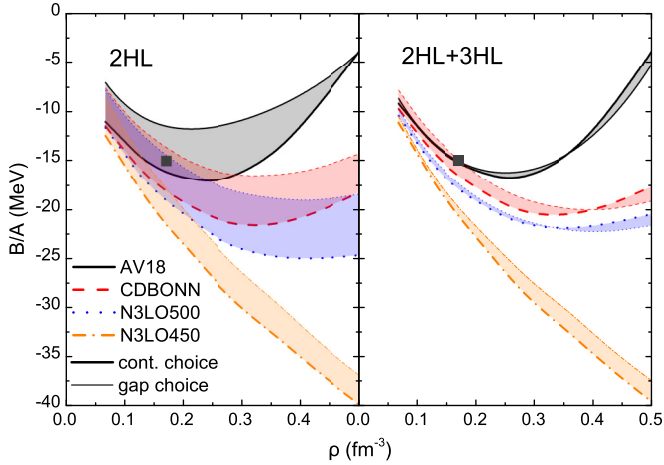
FIG. 2. Saturation curves of symmetric nuclear matter for different NN potentials in the 2HL (left panel) and 2HL + 3HL (right panel) approximations with continuous (bold curves) or gap-choice (thin curves) s.p. potentials. The markers indicate the empirical saturation point.

2HL (left panel) and 2HL + 3HL (right panel) levels with either continuous- (bold curves) or gap-choice (thin curves) s.p. potentials. As pointed out in Ref. [7], the saturation properties at the 2HL level are correlated with the strength of the hard core of the different potentials: hard potentials (AV18) saturate at lower densities and less binding energy than soft potentials (N3LO); however, in no case is satisfactory saturation obtained. Gap-choice results are substantially less attractive than continuous-choice results for all potentials.

Adding the 3HL results, the difference between gap and continuous choice decreases strongly, which indicates good convergence of the HLE, which should become independent of the choice of the s.p. potential at high enough order, as discussed before. It is also evident that the 3HL contributions with the more physical continuous choice are much smaller than the values with the gap choice such that the 2HL continuous-choice BHF results appear already close to convergence for all densities and potentials, in particular, the hard-core AV18 [22]. In fact the hatched areas between continuous- and gap-choice results can be taken as some convergence estimate of the HLE. In this spirit the worst convergence is exhibited by the N3LO450 model, which indeed has no hard core and is thus not expected to respect the HLE.

Nevertheless, nuclear matter saturation properties do not improve at third order for any potential. The reason is investigated in more detail in Fig. 3, which shows the individual continuous-choice total 3HL contributions E_3 [panel (a)] and the ratios $E_3/|E_2|$ [panel (b)]. One notes in the latter case that for all potentials the ratio remains well below 10% at any density, which again indicates good convergence of the HLE. From the density dependence of E_3 it becomes clear why the saturation properties do not improve: With the exception of the N3LO500 potential, all E_3's are decreasing functions of density at ρ_0 and therefore shift the saturation point to even higher densities.

Of further interest is also the comparison of $E_3/|E_2|$ with the HLE parameter κ [Fig. 3(d)], which governs the relative
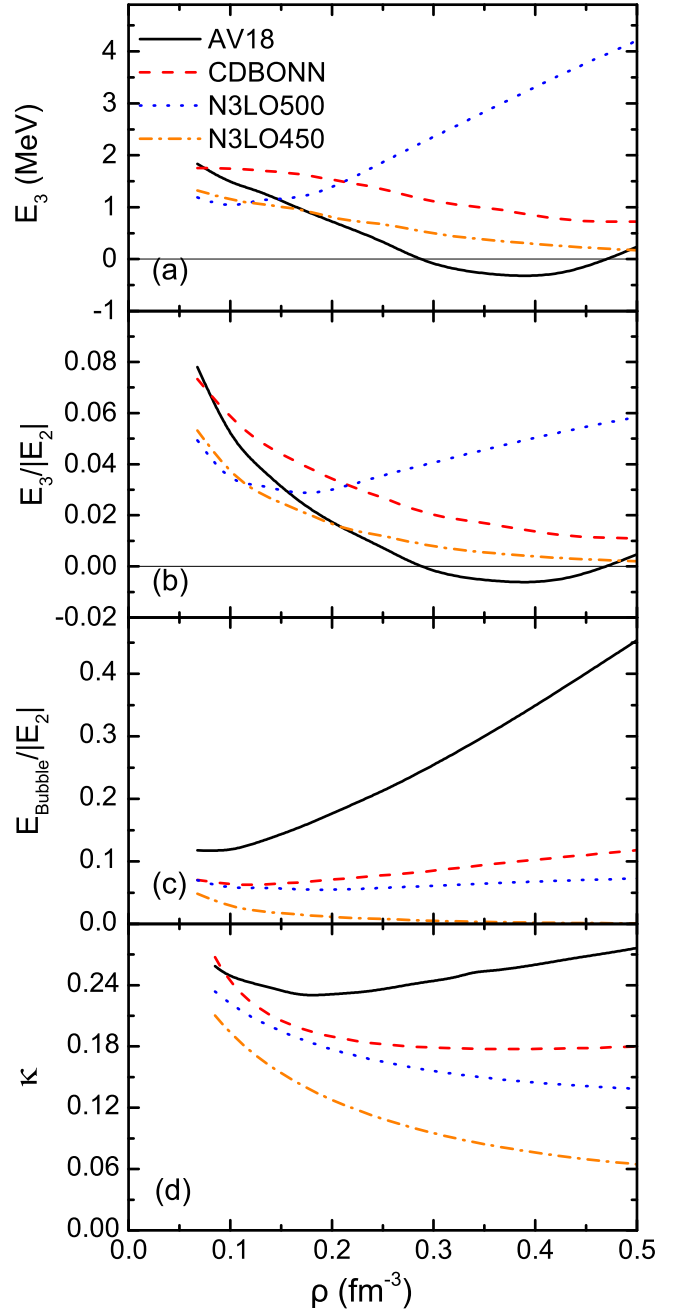

FIG. 3. (a) Continuous-choice 3HL contributions E_3 to the binding energy of SNM. (b) Ratio $E_3/|E_2|$ of 3HL-to-2HL contributions to the binding energy. (c) Ratio $E_{\rm Bubble}/|E_2|$. (d) Correlation parameter κ [7] of SNM as a function of density for different potentials.

size of the n and $n + 1$ cluster energies. We note that there is no clear correspondence between the magnitudes of κ and $E_3/|E_2|$ for the different potentials, e.g., the highest values of κ are obtained with the hard-core AV18 potential, but in this case $E_3/|E_2|$ becomes fairly small in a wide range of densities. Only for the extremely soft N3LO450 potential are both quantities consistently small due to the absence of a hard core.

The reason for this behavior is the fact that the total E_3 is the sum of the bubble, ring, and higher contributions,
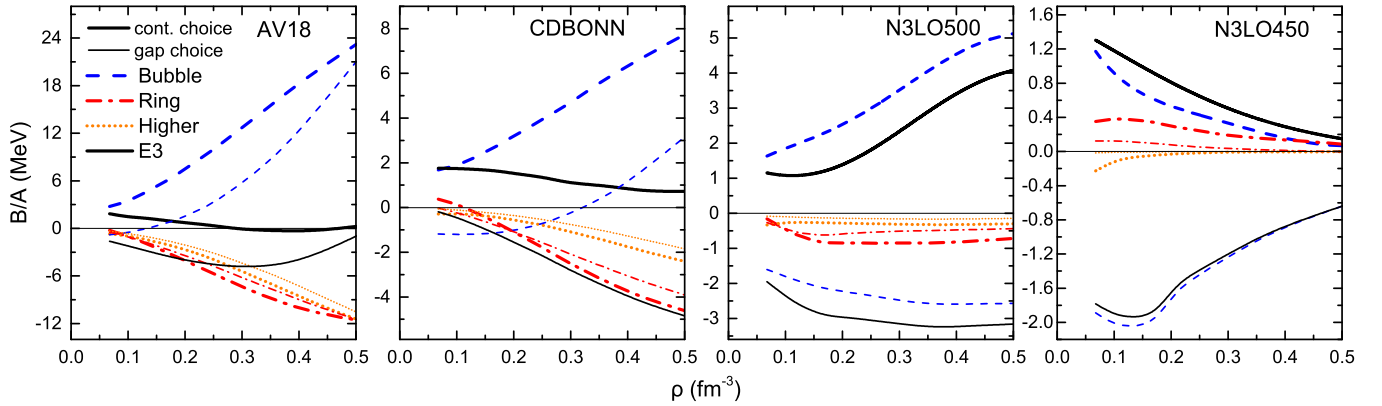
FIG. 4. Contributions of individual 3HL diagrams to the binding energy per nucleon, see Fig. 1: bubble [dashed lines, Fig. 1(c) + Fig. 1(d)], ring [dashed-dotted lines, Fig. 1(e)], higher-order [dotted lines, Fig. 1(f)], and total E_3 (solid lines) contributions with the continuous (bold curves) and gap (thin curves) choices for different potentials. Note the different energy scales.

which can be individually large and tend to cancel each other. This becomes clear in Fig. 3(c) where we plot only the contribution of the bubble diagrams, Fig. 1(c) + Fig. 1(d), to the convergence parameter $E_{\text{Bubble}}/|E_2|$. In this case the confrontation with κ is completely consistent according to the hard-core interaction strength, namely, in order AV18, CDBONN, N3LO500, and N3LO450.

In order to analyze this aspect in more detail, Fig. 4 shows the individual 3HL contributions for the different potentials and both gap and continuous choices. One should first note the rather different energy scales, reflecting again the strength of the short-range interaction. In most cases the total result E_3 is the sum of a positive bubble contribution and negative ring + higher contributions, which explains the small total value in the case of AV18, for example. In general the order of contributions is $|E_{\text{Bubble}}| > |E_{\text{Ring}}| > |E_{\text{Higher}}|$.

IV. CONCLUSIONS

We computed three-hole-line contributions to the binding energy of symmetric nuclear matter with frequently used modern NN potentials. In all cases the 3HL results obtained with the continuous choice of s.p. potentials are a small fraction of the 2HL values up to large densities such that the HLE seems to be well converged. This also is corroborated by the better agreement of gap- and continuous-choice results when including the relative 3HL contributions.

Nevertheless, the empirical saturation properties of nuclear matter are not reproduced for any potential, in particular, chiral forces with a small cutoff do not provide saturation at all. This means that very strong nuclear three-body forces are

required in order to achieve satisfactory saturation properties of nuclear matter. On the other hand, for these very soft potentials, the condition of a dominant short-range component of the interaction that is the very foundation of the HLE might be violated. In fact chiral potentials are devised to be employed in a perturbative framework, but it is nevertheless reassuring that 3HL results are small.

Indeed, once chiral three-body forces [26] are included consistently in the study of symmetric nuclear matter, their contribution does turn out to be large, and reasonable saturation properties can be obtained, subject to adjusting the relevant chiral parameters and cutoffs [4].

This paper dealt with the properties of infinite homogeneous nuclear matter. The question how this relates to the properties of finite nuclei [27] has also been investigated for a long time [28], in particular, in many recent works employing chiral forces [29], which is a field of current active research. We only note here that, due to the different ranges of the individual contributions to the correlation energy (e.g., BHF, bubble, ring, and higher diagrams), their importance and relative magnitudes in nuclear-matter or finite-nuclei calculations might be quite different [16].

[1] K. A. Brueckner and J. L. Gammel, Phys. Rev. **109**, 1023 (1958); J. P. Jeukenne, A. Lejeune, and C. Mahaux, Phys. Rep. **25**, 83 (1976); B. Day, Nucl. Phys. **A328**, 1 (1979).

[2] M. Baldo, *Nuclear Methods and the Nuclear Equation of State*, *International Review of Nuclear Physics Vol. 8* (World Scientific, Singapore, 1999).

[3] M. Baldo and G. F. Burgio, Rep. Prog. Phys. **75**, 026301 (2012).

[4] K. Hebeler, S. K. Bogner, R. J. Furnstahl, A. Nogga, and A. Schwenk, Phys. Rev. C **83**, 031301(R) (2011); Z. H. Li and H.-J. Schulze, *ibid.* **85**, 064002 (2012); L. Coraggio, J. W. Holt, N. Itaco, R. Machleidt, L. E. Marcucci, and F. Sammarruca, *ibid.* **89**, 044321 (2014); F. Sammarruca, L. Coraggio, J. W. Holt,

N. Itaco, R. Machleidt, and L. E. Marcucci, *ibid.* **91**, 054311 (2015); A. Carbone, A. Rios, and A. Polls, *ibid.* **90**, 054322 (2014); D. Logoteta, I. Vidaña, I. Bombaci, and A. Kievsky, *ibid.* **91**, 064001 (2015); M. Kohno, Prog. Theor. Exp. Phys. **2015**, 123D02 (2015); D. Logoteta, I. Bombaci, and A. Kievsky, Phys. Lett. B **758**, 449 (2016); Phys. Rev. C **94**, 064001 (2016).

[5] H. A. Bethe, B. H. Brandow, and A. G. Petschek, Phys. Rev. **129**, 225 (1963); B. H. Brandow, *ibid.* **152**, 863 (1966); M. W. Kirson, Nucl. Phys. **A99**, 353 (1967); B. D. Day, Rev. Mod. Phys. **39**, 719 (1967); R. Rajaraman and H. A. Bethe, *ibid.* **39**, 745 (1967).

[6] M. I. Haftel and F. Tabakin, Nucl. Phys. **A158**, 1 (1970); Phys. Rev. C **3**, 921 (1971); F. Coester, S. Cohen, B. Day, and C. M. Vincent, *ibid.* **1**, 769 (1970); B. D. Day and F. Coester, *ibid.* **13**, 1720 (1976).

[7] Z. H. Li and H.-J. Schulze, Phys. Rev. C **94**, 024322 (2016).

[8] R. B. Wiringa, V. G. J. Stoks, and R. Schiavilla, Phys. Rev. C **51**, 38 (1995).

[9] R. Machleidt, Phys. Rev. C **63**, 024001 (2001).

[10] D. R. Entem and R. Machleidt, Phys. Lett. B **524**, 93 (2002); Phys. Rev. C **68**, 041001(R) (2003); D. R. Entem, N. Kaiser, R. Machleidt, and Y. Nosyk, *ibid.* **92**, 064001 (2015); R. Machleidt, Symmetry **8**, 26 (2016).

[11] M. Baldo and H. R. Moshfegh, Phys. Rev. C **86**, 024306 (2012).

[12] B. D. Day, Phys. Rev. C **24**, 1203 (1981); Phys. Rev. Lett. **47**, 226 (1981).

[13] H. Müther and A. Polls, Prog. Part. Nucl. Phys. **45**, 243 (2000).

[14] W. H. Dickhoff and C. Barbieri, Prog. Part. Nucl. Phys. **52**, 377 (2004).

[15] M. Baldo, A. Polls, A. Rios, H.-J. Schulze, and I. Vidaña, Phys. Rev. C **86**, 064001 (2012).

[16] Y. Dewulf, W. H. Dickhoff, D. Van Neck, E. R. Stoddard, and M. Waroquier, Phys. Rev. Lett. **90**, 152501 (2003).

[17] B. D. Day, F. Coester, and A. Goodman, Phys. Rev. C **6**, 1992 (1972).

[18] B. D. Day and R. B. Wiringa, Phys. Rev. C **32**, 1057 (1985).

[19] H. Q. Song, M. Baldo, G. Giansiracusa, and U. Lombardo, Phys. Lett. B **411**, 237 (1997).

[20] R. Sartor, Phys. Rev. C **73**, 034307 (2006).

[21] H. Q. Song, M. Baldo, G. Giansiracusa, and U. Lombardo, Phys. Rev. Lett. **81**, 1584 (1998).

[22] M. Baldo, G. Giansiracusa, U. Lombardo, and H. Q. Song, Phys. Lett. B **473**, 1 (2000); M. Baldo, A. Fiasconaro, H. Q. Song, G. Giansiracusa, and U. Lombardo, Phys. Rev. C **65**, 017303 (2001).

[23] M. Baldo and C. Maieron, J. Phys. G **34**, R243 (2007).

[24] M. Baldo and C. Maieron, Phys. Rev. C **72**, 034005 (2005).

[25] K. Fukukawa, M. Baldo, G. F. Burgio, L. Lo Monaco, and H.-J. Schulze, Phys. Rev. C **92**, 065802 (2015).

[26] U. van Kolck, Phys. Rev. C **49**, 2932 (1994); E. Epelbaum, A. Nogga, W. Glöckle, H. Kamada, U.-G. Meißner, and H. Witała, *ibid.* **66**, 064001 (2002); P. Navrátil, Few-Body Syst. **41**, 117 (2007); J. W. Holt, N. Kaiser, and W. Weise, Phys. Rev. C **81**, 024002 (2010).

[27] B. H. Brandow, Rev. Mod. Phys. **39**, 771 (1967); H. S. Köhler, Phys. Rep. **18**, 217 (1975); H. Kümmel, K. H. Lührmann, and J. G. Zabolitzky, *ibid.* **36**, 1 (1978); E. Krotscheck, H. Kümmel, and J. G. Zabolitzky, Phys. Rev. A **22**, 1243 (1980).

[28] A. Kallio and B. D. Day, Nucl. Phys. A **124**, 177 (1969); H. Kümmel and J. G. Zabolitzky, Phys. Rev. C **7**, 547 (1973); J. G. Zabolitzky, Phys. Lett. B **47**, 487 (1973); Nucl. Phys. A **228**, 285 (1974); J. G. Zabolitzky and W. Ey, *ibid.* **328**, 507 (1979).

[29] S. K. Bogner, R. J. Furnstahl, and A. Schwenk, Prog. Part. Nucl. Phys. **65**, 94 (2010); N. Kalantar-Nayestanaki, E. Epelbaum, J. G. Messchendorp, and A. Nogga, Rep. Prog. Phys. **75**, 016301 (2012); J. E. Lynn, J. Carlson, E. Epelbaum, S. Gandolfi, A. Gezerlis, and A. Schwenk, Phys. Rev. Lett. **113**, 192501 (2014); G. Hagen, T. Papenbrock, M. Hjorth-Jensen, and D. J. Dean, Rep. Prog. Phys. **77**, 096302 (2014); A. Ekström, G. R. Jansen, K. A. Wendt, G. Hagen, T. Papenbrock, B. D. Carlsson, C. Forssén, M. Hjorth-Jensen, P. Navrátil, and W. Nazarewicz, Phys. Rev. C **91**, 051301(R) (2015); P. Navrátil, S. Quaglioni, G. Hupin, C. Romero-Redondo, and A. Calci, Phys. Scr. **91**, 053002 (2016); M. Piarulli, L. Girlanda, R. Schiavilla, A. Kievsky, A. Lovato, L. E. Marcucci, S. C. Pieper, M. Viviani, and R. B. Wiringa, Phys. Rev. C **94**, 054007 (2016); J. Simonis, S. R. Stroberg, K. Hebeler, J. D. Holt, and A. Schwenk, *ibid.* **96**, 014303 (2017).